One dimensional shallow foundation macro-element

M J Pender, Department of Civil & Environmental Engineering,
University of Auckland.

T B Algie, Partners in Progress Ltd., Sydney.

R Salimath, Tonkin and Taylor Ltd., Auckland.

L B Storie, Tonkin and Taylor Ltd., Auckland.

Abstract: Recently a number of macro-element models have been formulated for assessing the performance of shallow foundations during earthquake loading. These provide a computational tool that represents the nonlinear dynamic behavior of the foundation in a manner much simpler than finite element modelling; consequently, they are useful for preliminary design. The basis of this paper is the shallow foundation moment-rotation pushover curve, which is bracketed by the rotational stiffness at small deformations, determined by the small strain stiffness of the soil, and the moment capacity, which is a function of the soil shear strength and the vertical load carried by the foundation. Between these two limits there is a curved transition. The paper argues that when the vertical load carried by an embedded foundation is a small fraction of the vertical bearing strength, the moment-rotation behavior dominates the response. This means that the structure-foundation system can be reduced to a single degree of freedom (SDOF) model.

The form of the shallow foundation moment-rotation curve obtained from experimental and computational modelling is approximately hyperbolic; the nonlinear shape is due in part to the nonlinear deformation of the soil beneath the foundation but also to gradual loss of contact between the underside of the foundation and the soil below. The paper proposes a generalization of the pushover curve to give a shallow foundation cyclic moment-rotation relationship. The hysteretic damping properties of the model, as a function of the foundation rotation amplitude, are demonstrated as is the relation between secant stiffness and foundation rotation.

This paper shows how the model can be applied in numerical simulation of structure-foundation systems subject to earthquake time histories. The significance of the maximum displacement (foundation rotation) in relation to the damping and residual rotation at the end of the earthquake record are discussed.

1 Introduction

Background

A fundamental aspect of foundation behaviour is nonlinear interaction between the foundation and the surrounding soil. Often this interaction is idealised as elastic, but we must never overlook the fact that foundation-soil interaction is nonlinear. Having accepted this nonlinearity the problem is how to estimate the response of the foundation to imposed loading. There are well developed software systems that handle nonlinear behaviour which can also determine dynamic response. Thus our profession is well served with existing facilities. Unfortunately, there is an underlying problem in that the provision of numerical values for the various parameters required to make this numerical modelling possible is not a simple undertaking. Thus, from the point of view of foundation design, these highly sophisticated numerical tools may not be the best approach, at least for the initial stages of design. For most of the design process one needs simpler tools so that a number of scenarios can be evaluated quickly and the sensitivity of the response to variations in the input parameters assessed. At the final stage of the design process one might then want to use sophisticated numerical approaches to confirm the design decisions.

Macro-element idealisation

Recently a number of so-called macro-elements have been developed as an aid to the design of foundations to resist earthquake loading, Cremer et al. (2001) and (2002), Chatzigogos et al. (2007) and (2009), Figini et al. (2012), Gajan and Kutter (2008), Toh (2008) and Toh and Pender (2009). A macro-element is a computational tool that represents the behaviour of the foundation in a comparatively simple manner. If one was idealising foundation-soil interaction as linear, then an elastic macro-element would specify the vertical stiffness of the foundation, the horizontal stiffness and the rotational stiffness and any interaction between these stiffness parameters. In this way it is not necessary to model the distribution of stress and strain in the material beneath the foundation. This category of macro-element is well presented by Wolf and Deeks (2004). However, having said above that the soil behaviour is fundamentally nonlinear, alternative macro-elements, such as those cited above, are required. These are nevertheless quite sophisticated in that they employ the ideas of bounding surface plasticity using a bearing strength surface (the locus of all possible combinations of vertical load, horizontal shear, and moment – discussed further below) as the bounding surface. Nonlinear behaviour inside the surface is controlled by the distance between the current position on the action path and the bounding surface. Millen (2015) has implemented such a macro-element within the Ruaumoko, Carr (2016), nonlinear dynamic structural analysis software. Despite the success of these macro-elements, the behaviour of a very much simpler macro-element is explored herein.

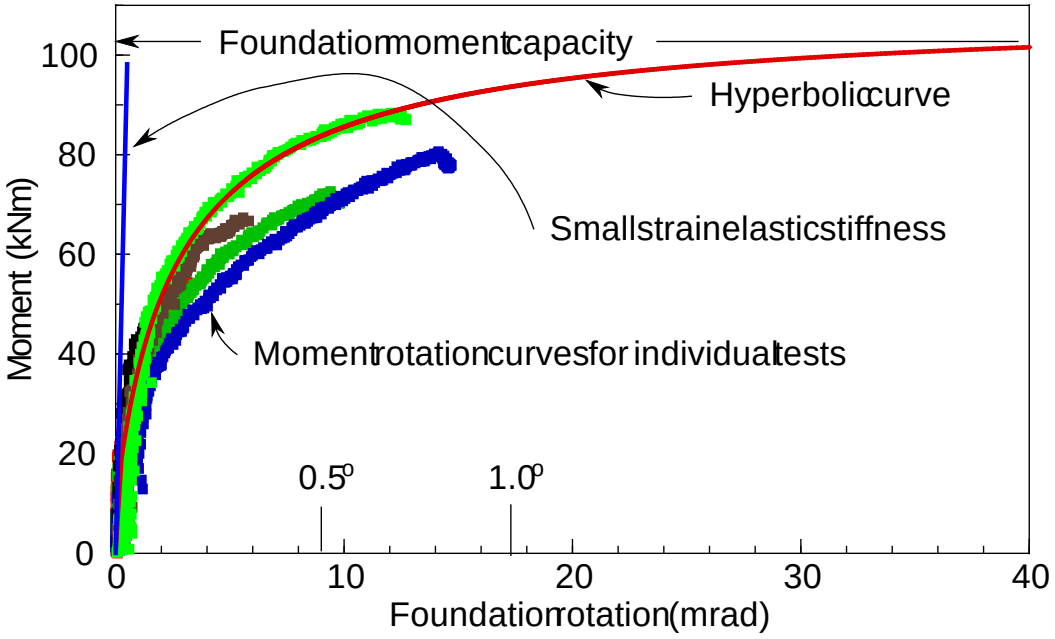

Figure 1 *Hyperbolic moment-rotation relation fitted to shallow foundation pull-back data (after Algie (2010).*

Measured shallow foundation response

Field experiments have been conducted a sites north of the Auckland CBD with shallow foundations supporting a simple single storey structure subject to gradual pull-back followed by snap-back release to; more details are given by Algie et al. (2010), Algie (2011), and Salimath (2017). The dynamic response of the system was recorded after each snap release. An added bonus was the static load-deflection curve obtained during the pullback phase of the test. The pullback response is in effect a static pushover curve for the foundation. Elsewhere, the relations between the rocking period and the pull-back angular displacement and damping and pull-back angular displacement are presented (Algie 2011).

The site used for the Algie tests had a profile of stiff cohesive soil. The soil profile was investigated with CPT tests between the surface and depth of 8 m. In some of these the shear wave velocity of the soil was measured which indicated a reasonably consistent shear wave velocity for the materials at the site equivalent to a small strain shear modulus of about 40 MPa.

Figure 1 shows some of the pull-back data obtained by Algie. It is apparent that there is considerable nonlinearity in the moment-rotation curves but a simple hyperbolic relationship, which asymptotes to the moment capacity of the foundation, can be fitted through the data. It is evident that some degradation occurs from one snapback to the next, particularly for those tests following the snapback which applies the largest moment to the system.

Further testing of this type was completed late in 2016 at Silverdale, a site further north of Auckland, the results are given by Salimath (2017). In this case

the shallow foundations were at the ground surface, whereas those for the Algie tests were embedded to a depth of 400mm. The Salimath tests, with foundation static load bearing strength factors of safety as high 10, left barely perceptible marking on the ground surface once the test rig was removed. This means that for these tests the nonlinearity in the moment-rotation curve was mostly a consequence of gradual loss of contact between the underside of the foundation and the foundation.

Simplification at large static factors of safety

An important control on foundation response under earthquake loading is the static bearing strength factor of safety. A common suggestion is that mobilising about one third of the vertical bearing strength of the foundation will give satisfactory static vertical load only performance (satisfactory is usually determined in relation to the settlement under working loads). However, often the actual mobilisation of bearing strength will be less, even considerably less, because of conservative decisions regarding design values for the soil parameters. Additionally, if there is a basement beneath the building, the area of the foundation may occupy the full plan area of the structure, in such cases the bearing pressure generated by the vertical load may be a very small fraction of the vertical bearing strength of the foundation. When this occurs there is unlikely to be settlement of the foundation under earthquake actions. Likewise there will be little horizontal displacement as the lateral stiffness of the foundation will be enhanced by the lateral stiffness generated by the sidewalls of the basement. In this way the response of the foundation under earthquake will be dominated by the nonlinear rotational stiffness of the foundation.

One dimensional macro-element proposed in this chapter

Following from the above paragraph this chapter explores the behaviour of a one dimensional macro-element in which there is no settlement or horizontal deformation of the foundation; the only deformation is nonlinear rotation. Modelling shallow foundations in this way reflects our observation, following the February 22, 2011 earthquake in Christchurch, of the apparently satisfactory performance of foundations for multi-storey buildings founded on gravel (Storie et al. (2015) and Storie (2017)).

The foundation supports a multi-storey elastic viscously damped structure which is represented as a concentrated mass supported on an elastic viscously damped column. As there is only one mass in the system the structure-foundation system is single degree of freedom (SDOF) model. It is intended that this will provide a simple method for foundation design sensitivity studies.

Substitute structure

The shape of the shallow foundation moment-rotation curve in Figure 1 is not unlike the moment-rotation curve for a reinforced concrete element. Figure 2 reproduces a diagram from the paper by Shibata and Sozen (1976). The procedure followed in this chapter is to make use of the ideas proposed by Shibata and Sozen, but to assume that the structural elements remain elastic

whereas the shallow foundation is the source of nonlinearity in the structure-foundation system. Figure 3, taken from Priestley et al. (2007), shows how the approach of Shibata and Sozen can be used to reduce a multi-storey frame structure to an equivalent SDOF model; they refer to this as a substitute structure. Priestley et al. explain how the parameters for the substitute structure, h_e, m_e, and K_e, can be evaluated.

One additional aspect needs to be included in the substitute structure model: the compliance of the soil beneath and adjacent to the foundation. This is done by representing the structure-foundation system as a SDOF elastic structure supported on a nonlinear rotational spring, which is discussed further below and illustrated in Figure 4a.

The essence of the Shibata and Sozen mechanism shown in Figure 2 is the development of hysteretic damping through ductile deformation of structural members. Priestley et al. explain that, for a given displacement of the SDOF mass, elastic soil structure interaction reduces the ductility demand in the structure; in effect this results in a reduction of the hysteretic damping of the system. As will be explained below nonlinear foundation behaviour develops hysteretic damping and so satisfactory response the structure-foundation system to earthquake excitation may still be feasible even through the above ground structure remains elastic.

Performance requirements

Prior to commencing the design of a foundation to resist earthquake loading performance criteria need to be specified. Since we are considering a one dimensional macro-element, this means specifying a permissible foundation rotation. After the Christchurch earthquake of February 2010 it was apparent that residual rotations of more than about 0.01 radian ($\approx$ 0.5 degrees) are easily perceived by the unaided eye. So if the design is based on a maximum rotation of 0.01 radian any residual rotation will not be readily visible. This is a conservative criterion as Deng et al. (2014) observed from centrifuge data that the residual rotation decreases as the pre-earthquake bearing strength static factor of safety increases. So for typical static design shallow foundation bearing strength factors of safety the post-earthquake residual rotation can be expected to be significantly less than the peak rotation during the earthquake. As will be seen below the one dimensional macro-element model shows hysteretic damping even at small foundation rotations.

Foundation bearing failure

There have been many proposals for the design of shallow foundations pointing out that brief instances of bearing failure during the earthquake response are unlikely to generate significant permanent deformations but the transient reduction in stiffness will lead to a reduction in earthquake actions, for example: Anastasopoulos et al. (2010) and (2014), Gajan et al. (2008), Gazetas (2015), Loli et al. (2015), Pecker and Teyssandier (1998), and Pender (2007). Although this is a convincing idea within the geotechnical community it is not readily accepted by the structural engineering fraternity who have a preference for

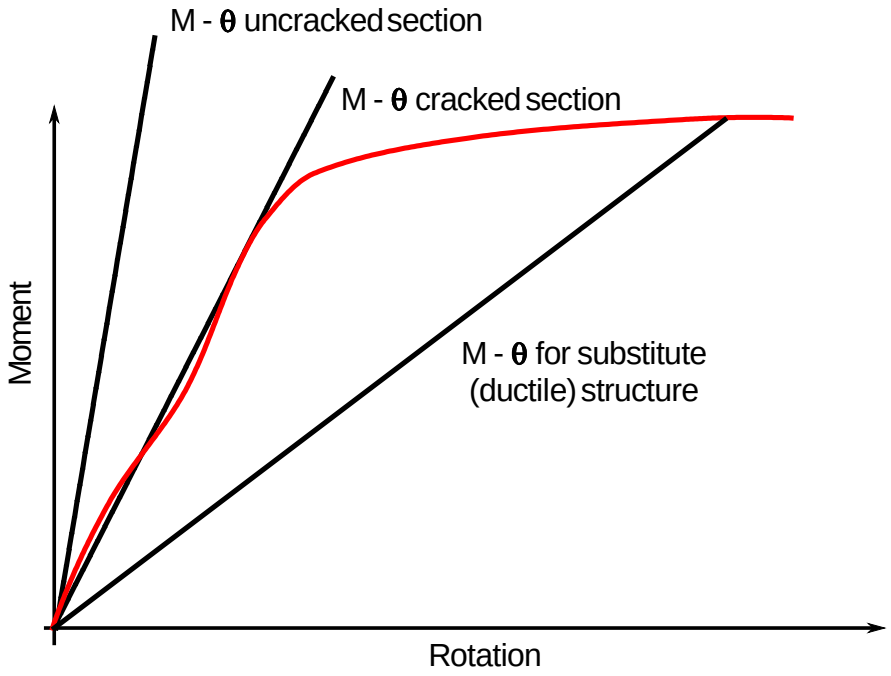

Figure 2 *The basis of Shibata and Sozen's substitute structure concept.*

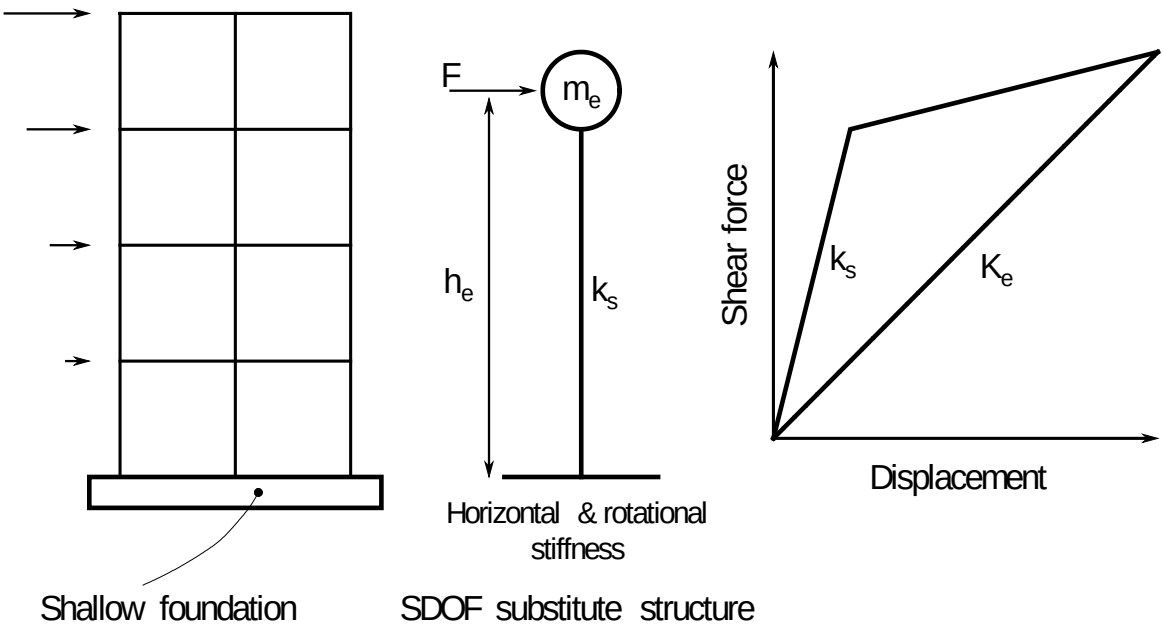

Figure 3 *Implementation of the substitute structure concept as presented by Priestley, Calvi and Kowalsky (2007).*

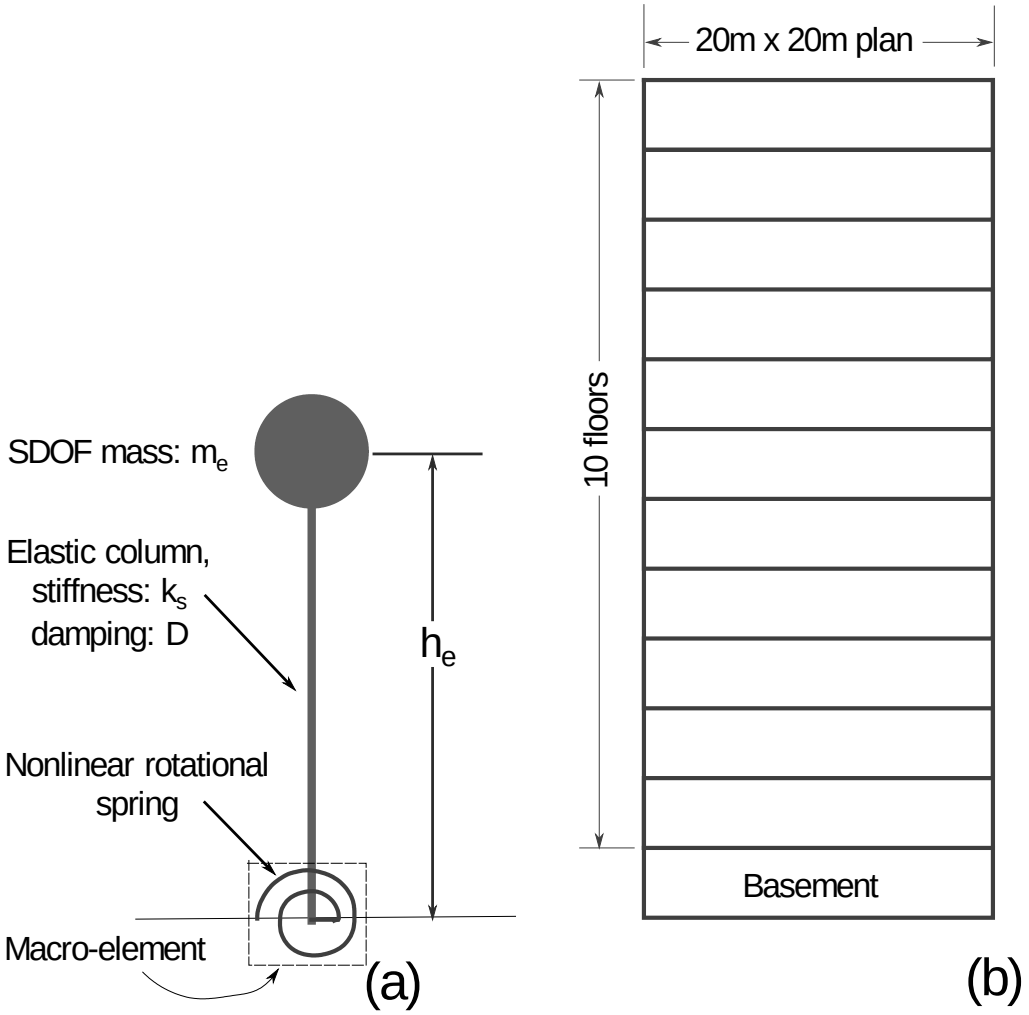

Figure 4 *Single degree of freedom model of the 10 storey building with one basement level founded in dense gravel; (a) SDOF model, (b) actual structure.*

restricting nonlinear deformations to above-ground structural members (a notable exception being Kelly (2009)). As will be seen below limiting the maximum foundation rotation to less than about 0.01 radians will provide benefits from nonlinear response but will still be well short of mobilising the moment capacity of the foundation, that is brief instances of bearing failure are unlikely at such modest rotations. Panagiotidou et al. (2012) found that for shallow foundations on stiff clay the onset of P-delta effects, which reduce the moment capacity of the system, occurs at rotations between 0.01 and 0.02 radians. Thus specifying a small value for the maximum design rotation has the added advantage that P-delta effects will not reduce the system capacity.

2 Equations of motion

Wolf (1985), in his book *Dynamic Soil-Structure Interaction,* develops the equations of motion for a single degree of freedom model in which a lumped mass is positioned at some distance above a foundation resting on an elastic medium with radiation damping. There are three components to horizontal the

displacement of the SDOF mass: the horizontal displacement of the foundation, the rotation of the foundation multiplied by the height of the mass, and the flexural displacement of the column supporting the mass, but since there is one mass in the system there is only one dynamic degree of freedom. Wolf shows how the different stiffness components contribute to the natural frequency of the structure-foundation system with the following equation:

$$\omega_e^2 = \frac{\omega_s^2}{1 + \frac{k_s}{k_h} + \frac{k_s h_e^{\,2}}{k_\varphi}} \qquad (1)$$

where: ω_e and ω_s are respectively the natural frequencies of the elastic structure-foundation system and the fixed base structure,
k_s is the flexural stiffness of the column supporting the SDOF mass,
k_h is the lateral stiffness of the foundation,
k_φ the rotational stiffness of the foundation,
and h_e is the height above foundation level of the SDOF lumped mass (m_e).

This equation shows that inclusion of foundation compliance reduces the natural frequency (lengthens the natural period) of the structure-foundation system. Equation (1) assumes that all stiffness components are elastic and gives the natural frequency of the system under steady state sinusoidal excitation, but in our case the foundation rotational stiffness is nonlinear so the natural frequency of the system under steady state excitation is variable being a function of the rotational amplitude of the foundation.

In this chapter we consider embedded foundations for which the lateral stiffness is large and does not have a significant effect on the system natural frequency given by the above equation. Consequently, the lateral stiffness of the foundation will not be included in the modelling below.

Under earthquake excitation the response is not steady state and so the rotational stiffness of the foundation, derived from the hyperbolic moment-rotation relationship, will vary from time step to time step. This means that the equation of motion for the SDOF mass needs to be integrated incrementally, the incremental equation of motion is:

$$m_e \Delta\ddot{u}_m + D\Delta\dot{u}_m + K_e(\varphi)\Delta u_m = -m_e \Delta\ddot{u}_g \qquad (2)$$

where: m_e is the SDOF mass (tonnes),
D is the parameter for the equivalent viscous damping ratio of the column supporting the SDOF mass (tonnes/sec),
φ is the foundation rotation (radians)
$K_e(\varphi)$ is the equivalent system stiffness which includes the contribution from the foundation moment-rotation curve and the lateral stiffness of the column (kN/m),
$\Delta\ddot{u}$, $\Delta\dot{u}$, and Δu are respectively the horizontal acceleration increment, velocity increment, and displacement increment of the SDOF mass,

$\Delta\ddot{u}_g$ is the increment in input acceleration (m/sec^2).

Note that the velocity dependent damping term in equation (2) comes from the elastic column supporting the SDOF mass a distance h_e above the foundation level. All the foundation damping comes from hysteretic moment-deformation loops which are implicit in the foundation moment-rotation relationship discussed below. Frequency dependent elastic radiation damping is the usual energy dissipation mechanism used in elastic soil structure interaction. However, it is well known that elastic radiation damping for foundation rotation is very small so the hysteretic action is very important during foundation rocking.

The equivalent stiffness of the structure foundation system including the effect of the flexural stiffness of the column and the nonlinear rotational stiffness of the foundation is:

$$K_e(\varphi) = \frac{k_s K(\varphi)}{K(\varphi) + h_e^2 k_s} \tag{3}$$

where: $K(\varphi)$ is tangent rotational stiffness of the foundation at the current value of φ.

A possible extension of the above approach would be to include the mass and rotational inertia of the foundation. Doing this means that the structure-foundation system now has three dynamic degrees of freedom (lateral inertial displacement of the mass at a height h_e above foundation level, and lateral inertial displacement of the foundation, and inertial rotation of the foundation). Wolf (1985) states that pursuing this analysis does not produce results significantly different from those obtained with the SDOF model. Using modal analysis it is found that the two additional periods are well removed from that of the SDOF model and the first mode frequency is hardly different from that for the SDOF model. However, there is one significant factor in which the mass of the foundation block is important; the increased vertical load on the foundation enhances the moment capacity.

3 Foundation moment capacity

Definition of the nonlinear moment-rotation behaviour of the foundation is needed to calculate the response of the SDOF macro-element system to earthquake input. This is defined by two limiting conditions – the linear stiffness at very small rotations and the ultimate moment capacity of the foundation under the fixed vertical load. This section covers the estimation of the foundation moment capacity using the bearing strength surface.

Bearing strength surface

The following equation gives the standard estimation of the bearing strength of a shallow foundation under vertical load, horizontal shear, and moment:

$$q_u = c\lambda_{cs}\lambda_{cd}\lambda_{ci}N_c + q\lambda_{qs}\lambda_{qd}\lambda_{qi}N_q + \frac{1}{2}\gamma B\lambda_{\gamma s}\lambda_{\gamma d}\lambda_{\gamma i}N_\gamma \quad (4)$$

where: λ_{cs}, λ_{qs}, and $\lambda_{\gamma s}$ are shape factors;
λ_{cd}, λ_{qd}, and $\lambda_{\gamma d}$ are depth factors;
λ_{ci}, λ_{qi} and $\lambda_{\gamma i}$ are inclined load factors;
and c, q, q_u, B, N_c, N_q and N_γ have their usual meanings.

A set of shape, depth, and inclined load factors for use in equation (4) are given by Pender (2017). Equation (4) provides a way of estimating what combinations of vertical load, horizontal shear, and moment mobilise all the available shear strength of the soil underlying and surrounding a shallow foundation. The locus of these combinations forms a three dimensional *Bearing Strength Surface* (BSS). There are two surfaces to consider, generated using appropriate rearrangements of equation (4), one for the undrained case and another for the drained case.

A convenient way of presenting the surfaces is to use axes defined in terms of dimensionless parameters, one for vertical load, another for horizontal shear, and a third for moment applied to the foundation. The normalising parameter is the ultimate bearing strength of the foundation subject to vertical load only; a possible suite of dimensionless parameters is then:

$$Vn = \frac{V}{V_{uo}} \qquad Hn = \frac{H}{V_{uo}} \qquad Mn = \frac{M}{BV_{uo}} \quad (5)$$

where: V, H and M are actions applied to the foundation,
Vn, Hn and Mn are normalized foundation actions,
B is the width of the foundation,
V_{uo} is the ultimate vertical load capacity of the foundation in the absence of shear and moment.

The Vn, Hn and Mn notation refers to general foundation actions. When referring to a bearing strength ultimate limit state we will use the notation Vnu, Hnu and Mnu.

When only vertical actions are to be applied to the foundation the usual terminology is to refer to the bearing capacity which has units of pressure (q_u in equation (4)). When the vertical load is accompanied by shear and moment it is helpful to speak of bearing strength (q_u times the effective contact area) which has units of force rather than pressure; this terminology is used in the remainder of the paper.

Views of the upper halves of the two versions of the surface are shown in Figures 4 and 5. Algebraic equations for the bearing strength surfaces, developed from equation (1), are given by Pender (2017).

The bearing strength surfaces show that the capacity of a shallow foundation is not a single number but the combination of the vertical load, horizontal shear force and moment where the action path (a plot of the combinations of vertical

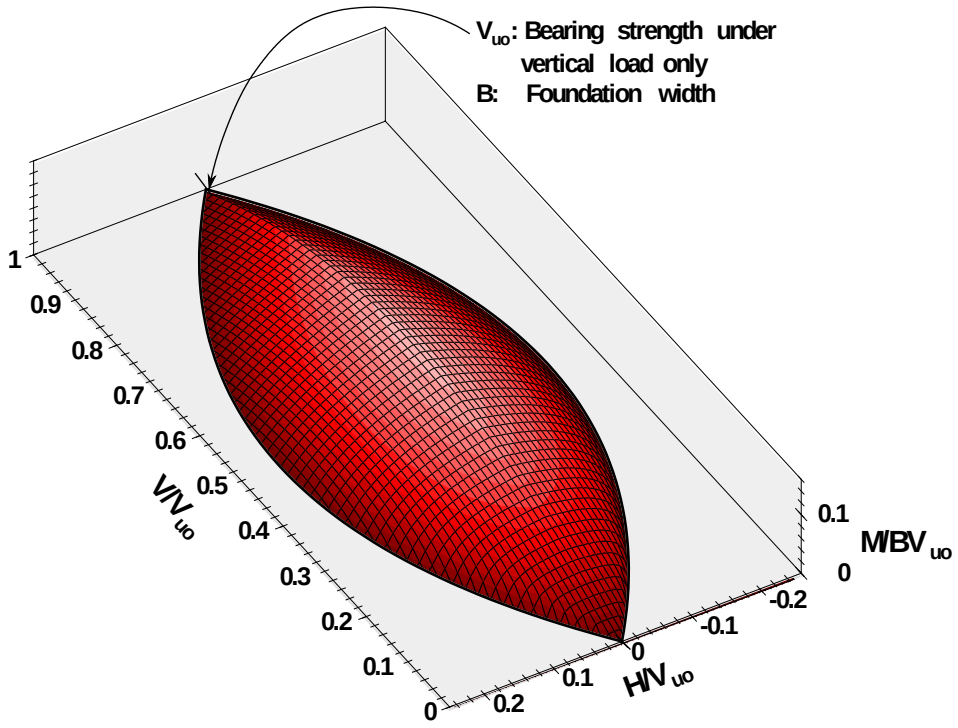

Figure 5. *Undrained bearing strength surface for a surface strip foundation.*

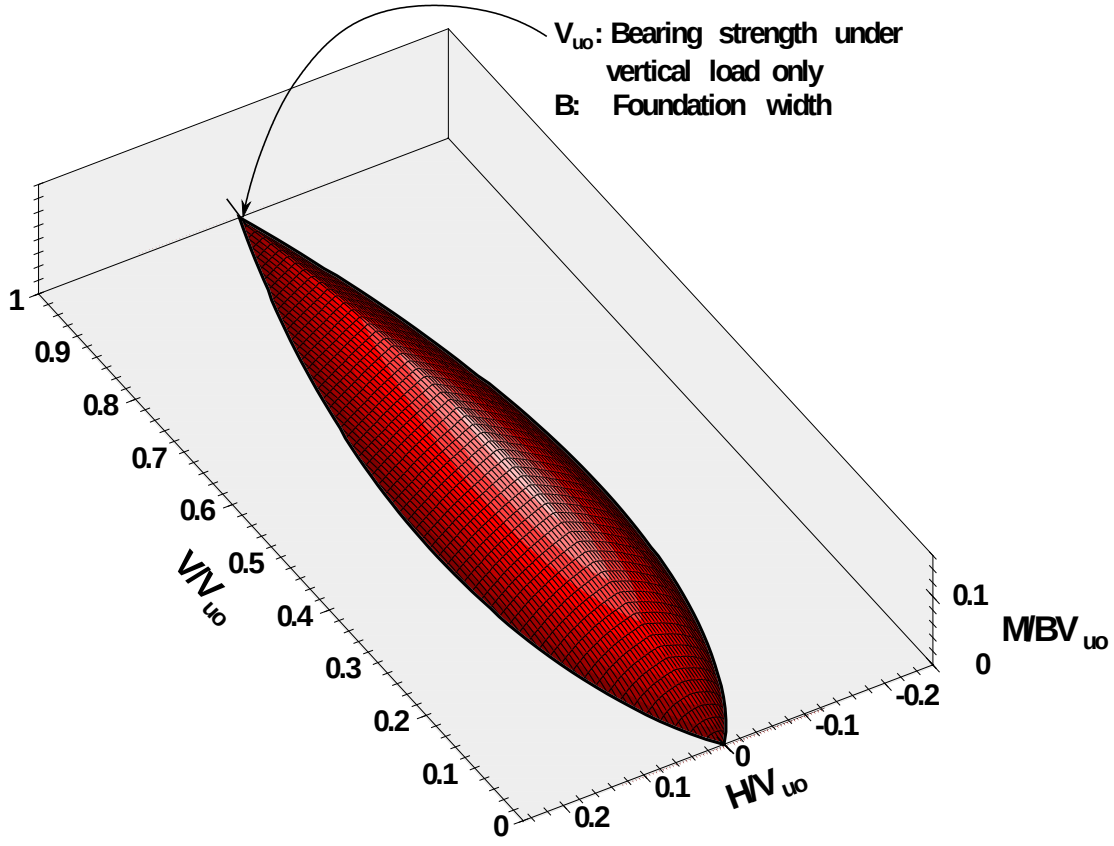

Figure 6. *Drained bearing strength surface for a surface strip foundation.*

load, horizontal shear and moment applied to the foundation) intersects the bearing strength surface.

Moment capacity at constant vertical load with moment and shear
Estimation of the moment capacity of the foundation must consider the action path applied to the foundation, in our case the vertical load is constant so, in effect, we need to consider a Vn constant section through the BSS. In addition, to obtain the moment capacity of the foundation the solution process must allow for the dependence of eight of the nine λ factors ($\lambda_{\gamma d}$ is independent of moment as it has the value of unity) on the effective foundation width, B′, and this in turn is a function of the unknown ultimate moment. The inclined load terms, λ_{ci}, λ_{qi} and $\lambda_{\gamma i}$, are functions of the horizontal shear as well as B′, but the ultimate shear can usually be expressed as a multiple of the ultimate moment as the SDOF shear force is applied some distance above the foundation and so produces the foundation moment. Consequently we have an equation, albeit a rather complex one, for one unknown, the ultimate moment capacity under the fixed vertical load V:

$$\left\{\begin{array}{l} cN_c\lambda_{cs}(M_u)\lambda_{cd}(M_u)\lambda_{ci}(M_u) \\ \qquad + qN_q\lambda_{qs}(M_u)\lambda_{qd}(M_u)\lambda_{qi}(M_u) \\ \qquad\qquad + \frac{1}{2}\gamma B'(M_u)N_\gamma\lambda_{\gamma s}(M_u)\lambda_{\gamma i}(M_u)\lambda_{\gamma d} \end{array}\right\} B'(M_u)L - V = 0 \qquad (6)$$

The solution to equation (6) gives the moment at which the effective width of the foundation is reduced to the extent that the value of q_u times the effective area of the foundation is equal to the applied vertical load.

4 Foundation hyperbolic moment-rotation relationship

Figure 1 presents the static moment-rotation curves obtained during the application of the pullback forces to one of the foundation sets at the Albany site. A hyperbolic curve is seen to fit through the data.

Hyperbolic curves have been used to approximate the stress-strain behavior of soil elements since the work of Kondner (1963). Duncan and Chang (1970) applied this model in finite element analysis. It is not surprising that a similar relation applies to shallow foundation behavior as the foundation response is the integration of the responses of a large number of soil elements each of which follows an approximately hyperbolic relationship. In this way it is possible to argue, heuristically, that the overall response of the foundation will be similar to that of the individual elements.

The form of the hyperbolic relationship shown in Figure 2 is:

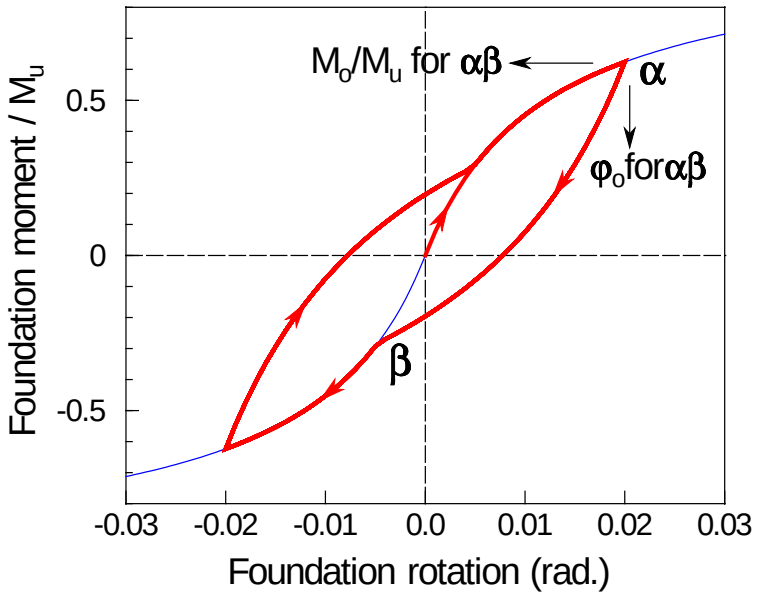

Figure 7 *Cyclic hyperbolic moment-rotation curve with the definition of the M_o and φ_o parameters.*

$$M = \frac{\varphi}{\frac{\Lambda}{K_{\varphi i}} + \frac{\Omega \varphi}{M_u}} \tag{6}$$

where: M and φ are the current foundation moment and rotation respectively,
$K_{\varphi i}$ and M_u are the initial rotational stiffness and moment capacity of the foundation respectively,
and Λ and Ω are numerical parameters that may be used to refine the fit of the curve to the data (the curve fit in Figure 1 has a value of unity for both of these parameters).

Salimath (2017) found that values for Λ and Ω depend on the shape of the foundation. The parameter Λ also has an effect on the amount of hysteretic damping in the cyclic hyperbolic relationship which is discussed below.

Equation (6) provides a pushover curve for a shallow foundation, which is bounded by the moment capacity of the shallow foundation at large values of the rotation and the elastic rotational stiffness at small rotations.

Equation (6) also acts as a backbone curve for the extension of hyperbolic relationship to cyclic loading given by the following equation:

$$M = \frac{K_{\varphi i}\left(AM_u - M_o\right)\left(\varphi - \varphi_o\right)}{\Lambda\left(AM_u - M_o\right) + \Omega K_{\varphi i}\left(\varphi - \varphi_o\right)} + M_o \tag{7}$$

where: M_o and φ_o are the initial values for the current branch of the moment-rotation curve(defined in Figure 7),

and A takes values of +1 and -1 indicating if the foundation is being loaded towards the moment capacity M_u or $-M_u$.

Whenever an unloading or reloading loop intersects the backbone curve the moment-rotation response then follows the backbone curve (this prevents the system developing unreasonably large foundation rotations). When the direction of loading reverses the stiffness reverts to the rotational stiffness at zero moment, $K_{\varphi i}$. The moment capacity can be reached when the rotation is to the left or the right, so that M_u limits the moment to the right and $-M_u$ limits it to the left. Figure 7 shows how equation 7 extends the pushover curve to give the cyclic response of a shallow foundation.

The rotational stiffness of the foundation is given by the slope of the current branch of the hysteretic moment-rotation loop and, as in apparent from Figure 7, the slope of the M-φ curve changes continuously with moment. Because of this continuous variation in stiffness the nonlinear moment-rotation relationship is not associated with plastic yielding but rather is a type of hypoplasticity.

Equations 6 and 7 are relatively simple expressions representing complex behavior. Spring bed models indicate, for a shallow foundation under a fixed vertical load and gradually increasing moment, that there will be a gradual loss of contact at the edge of the foundation. The macro-element models of Cremer et al. and Chatzigogos et al. incorporate this effect specifically, but herein it is assumed that uplift effects are handled implicitly and part of the reason for the shape of the moment-rotation curve is a consequence of the reduction of contact area. Salimath (2017) reports on an extensive series of finite element analyses, using Plaxis 3D, (Plaxis 2012) which have a rigid rectangular foundation, under constant vertical load, on a clay soil with a no-tension interface between the foundation and the underlying clay. This modelling confirms that a hyperbolic curve is a reasonable representation of the shallow foundation moment-rotation push-over curve when uplift occurs.

5 Rotation dependent foundation stiffness and hysteretic damping

Elastic soil-structure interaction modelling relies on radiation damping to take vibration energy away from the foundation. However, for rotation of the foundation damping available from elastic radiation is small. Consequently, herein we assume that all the foundation damping is derived from the area of the hysteresis loops. Figure 8 shows that the hysteretic damping increases as the rotation amplitude increases. The apparent foundation rotational stiffness and the equivalent viscous damping ratio associated with a given hysteretic moment-rotation loop are defined in Figure 10a. Figure 10b gives the variation of the rotational stiffness with the logarithm of the rotation amplitude. Figure 10c gives the variation of the hysteretic damping against the logarithm of the rotation amplitude. When the rotation amplitude is 0.05 the hysteretic damping is 28%. Ishihara (1996) states that the maximum damping ratio for the hyperbolic model is 64%. Clearly the damping in the present model does not

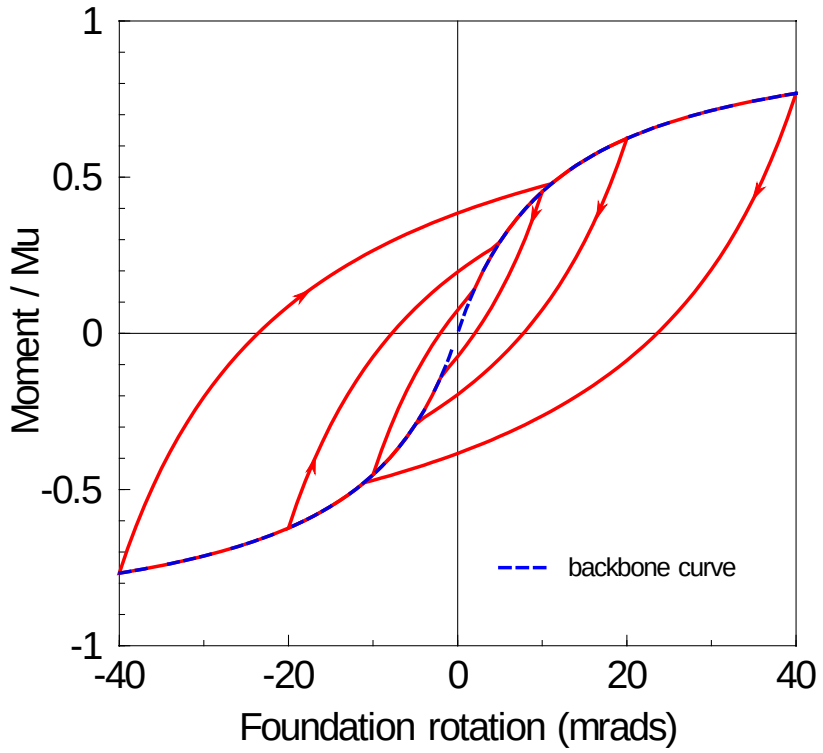

Figure 8 *Steady state hysteretic shallow foundation moment-rotation loops with the Λ parameter set to 1.0.*

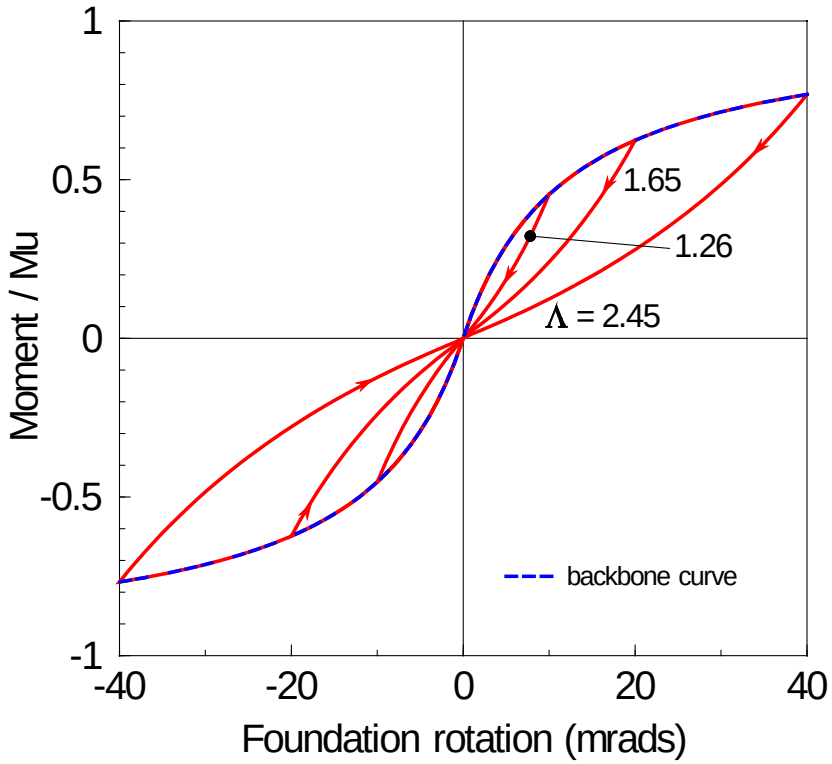

Figure 9 *Steady state hysteretic shallow foundation moment-rotation loops with the Λ parameter varied at each turning point so that the loops pass through the origin.*

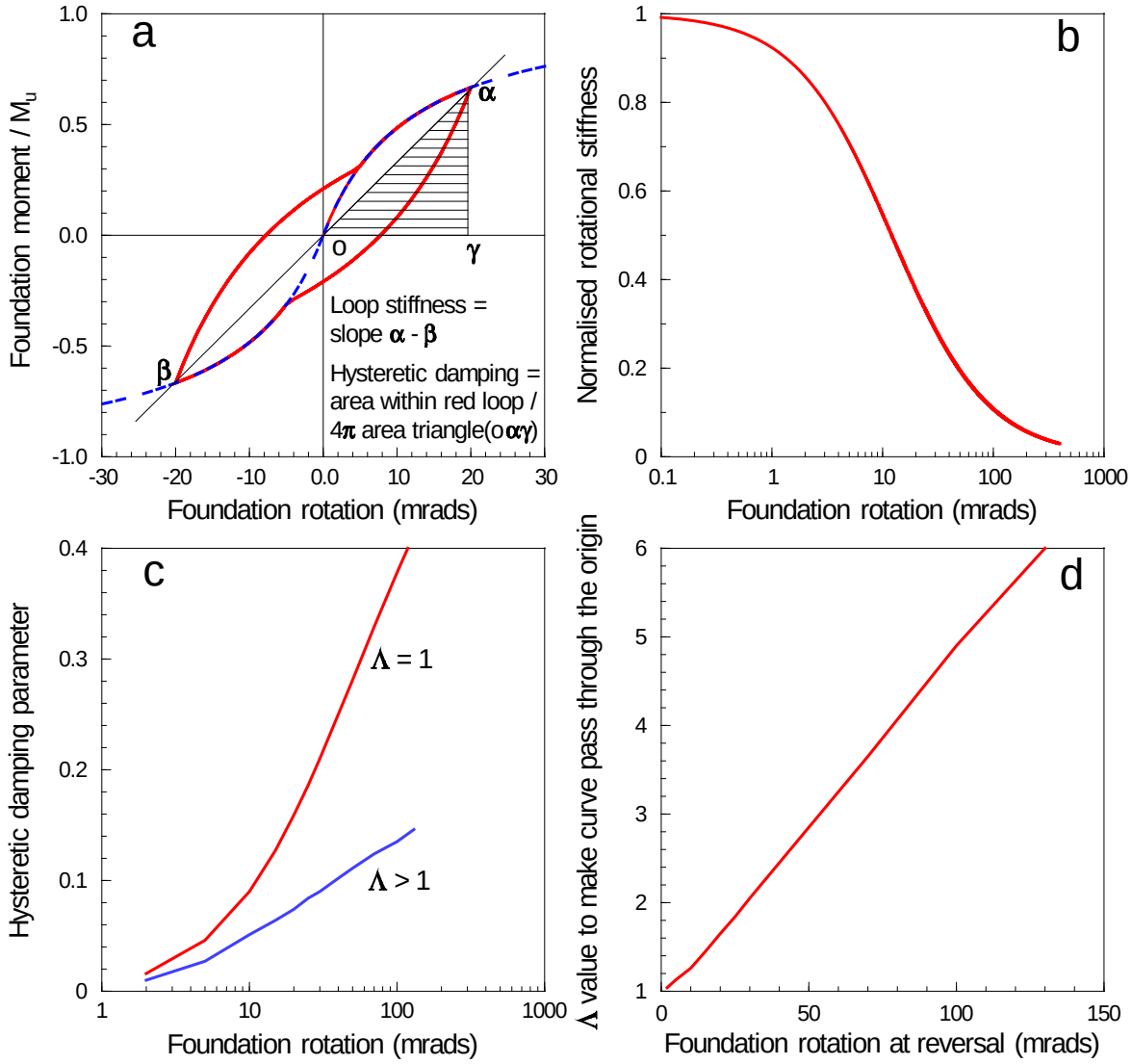

Figure 10 *Hysteretic equivalent viscous damping ratio and apparent rotational stiffness as functions of foundation rotation amplitude. (a) parameter definitions; (b) foundation rotational stiffness as a function of rotation amplitude; (c) damping ratios against rotation amplitude; (d) value of the parameter Λ required to get the loops to pass through the origin as a function of rotation at the turning point.*

approach such a value at likely rotation amplitudes, a consequence of the hysteretic loops reattaching to the backbone curve rather than crossing it.

All the moment-rotation loops in Figure 8 are generated with the Λ parameter set to a value of 1.0. The amount of damping can be reduced by decreasing the rotational stiffness of the foundation immediately after a change in direction of rotation which is achieved if Λ is given a value greater than unity. The effect of doing this is shown in Figure 9 where the values of Λ have been adjusted so that the hysteresis loops pass through the origin.

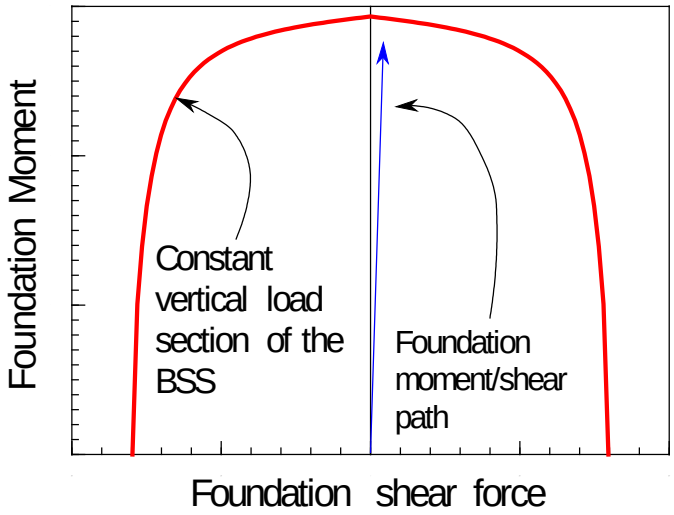

Figure 11 *Constant vertical load section of the bearing strength surface showing the path for foundation actions.*

As the foundation rotation increases the slope of the line between the end points of the hysteresis loops in Figures 8 and 9 decreases; this gives the relationship, for the backbone curve, between the apparent rotational stiffness of the foundation which is plotted in Figure 10b.

6 Example calculations

In this section the response to earthquake excitation of a 10 storey building with a single level basement and a foundation with a hyperbolic moment-rotation properties is presented. The input is the acceleration recorded in the 1940 El Centro earthquake (the N-S component) adjusted to a peak ground acceleration of 0.3g. The nonlinear response of the structure-foundation system was calculated to the 0.3g El Centro record scaled with factors of 0.5, 1.0, 2.0 and 3.0. The algorithm presented in chapter 7 of Clough and Penzien (1993), for calculating the incremental response of a nonlinear single degree of freedom system, was used in these computations. In addition the response of the system when the foundation behaves elastically was evaluated. All the time history and response spectra calculations discussed in this chapter were done using Mathcad 15 (PTC 2016). The earthquake acceleration histories had a time step of 0.02 seconds.

The details of the 10 storey building are shown in Figure 4b, the plan dimensions are 20 m by 20 m. The damping ratio for the elastic building structure was set at 3% of the critical damping value. The building is founded on dense dry gravel with an angle of shearing resistance of 45 degrees and a shear wave velocity of 280 m/sec. The conversion from the actual structure, Figure 4b, to the SDOF model, Figure 4a, was done by assuming a uniform distribution of mass with height in the building and setting the SDOF mass to 70% of the total mass acting at 70% of the building height.

Figure 11 gives a cross-section of the bearing strength surface at the vertical load imposed by the gravity loading (assumed constant during the earthquake). Also shown in Figure 11 is the shear – moment action path for the foundation; because of the height of the SDOF mass the action path is close to vertical so the moment capacity of the foundation is close to the top of the section of the BSS.

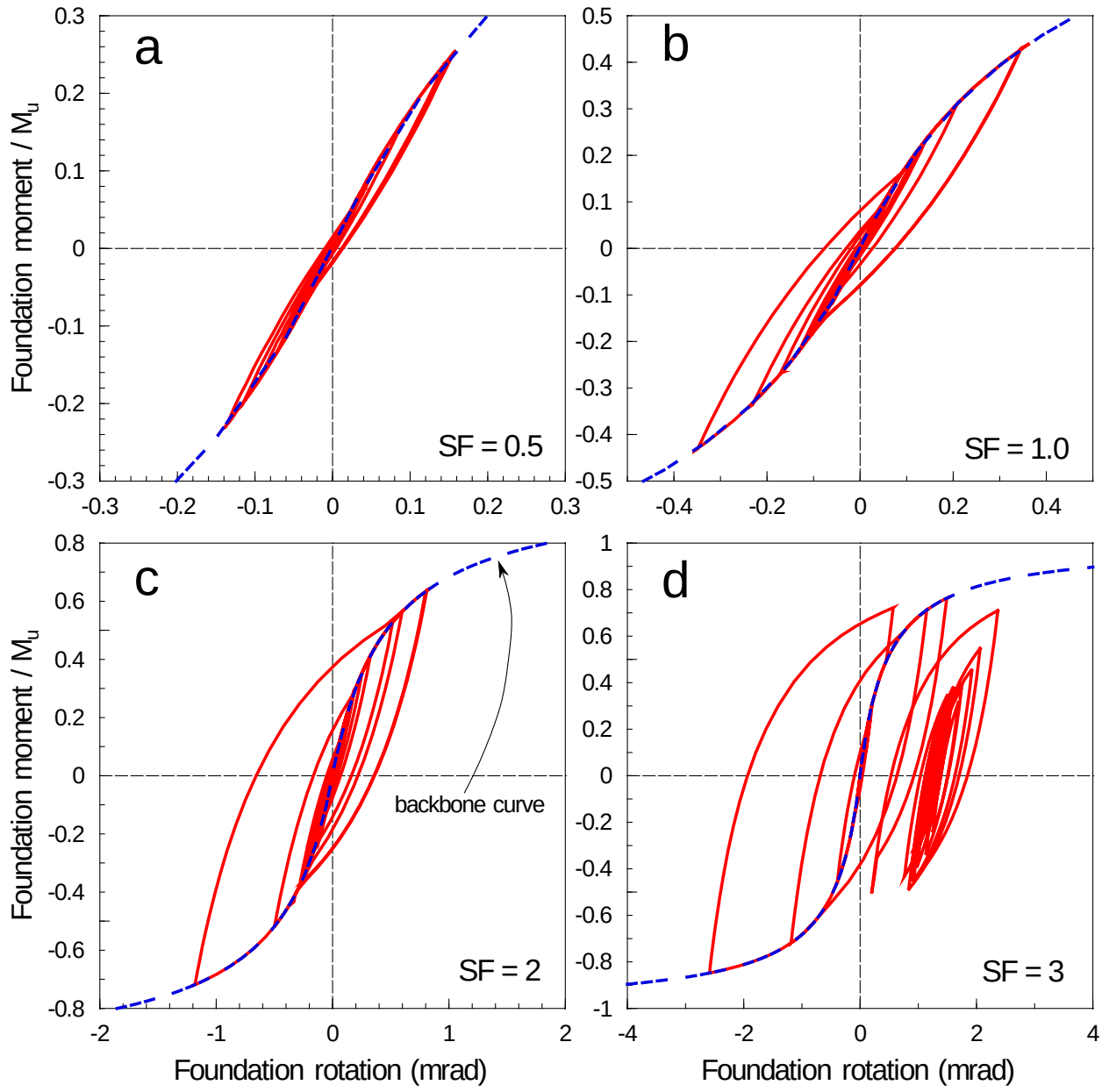

Figure 12 *Foundation moment-rotation loops calculated during the response to scaled El Centro ground acceleration input motions.*

The calculated foundation moment-rotation loops are plotted in Figure 12. These show increasing hysteretic damping as the scale factor applied to the input motion is increased. Figure 13 shows the variation of the foundation tangent rotational stiffness, normalised with respect to the small rotation value ($K_{\varphi i}$), for the first 8 seconds of the response when the scale factor is 2.0 (the vertical lines indicate the abrupt change in stiffness when the direction of motion is reversed as then the rotational stiffness reverts to the small rotation value).

Figure 14 has the response spectra for the outputs from the scaled input motions, the spectra were obtained by processing the calculated horizontal acceleration histories of the SDOF mass. In addition there is a spectrum for the response when the foundation behaves elastically. All spectra were calculated for

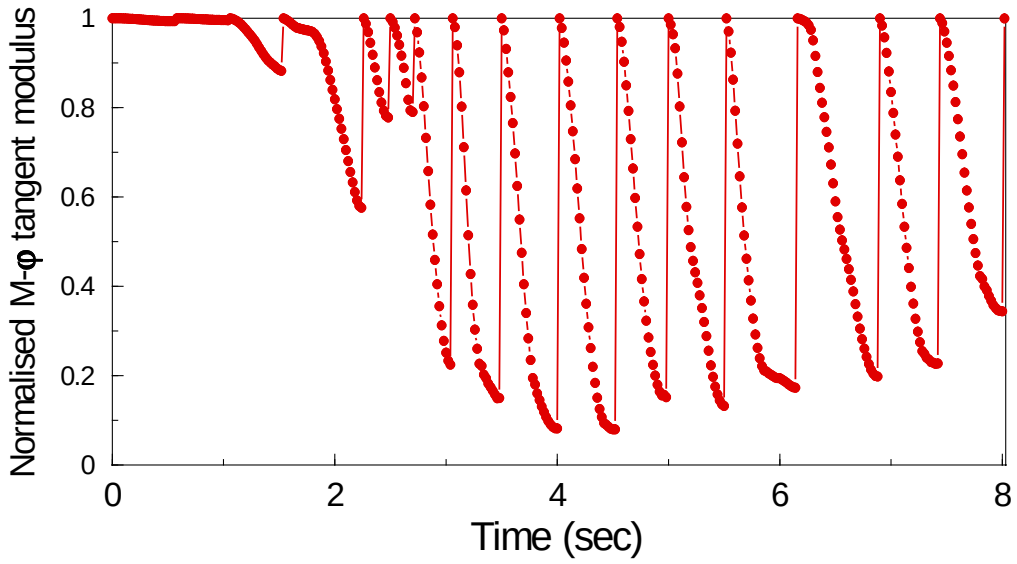

Figure 13 *Variation of the foundation tangent rotational stiffness during the first 8 seconds of the response to the El Centro input with a scale factor of 2.0. (The vertical lines indicate turning points when the foundation rotational stiffness reverts to the initial small rotation value.)*

a damping ratio of 5% and the plotted spectral accelerations are normalized with respect to the peak input acceleration for the scaled input, so the ordinates in Figure 14 are dimensionless. It is apparent that the peak response in all cases occurs at a period close to 1 second, the natural period of the above ground part of the structure-foundation system. As the scaling of the input motion increases there is more hysteretic damping generated by the foundation as evidenced by the moment-rotation loops in Figure 12. The effect of this is that the spectral peaks in the responses of the SDOF mass are reduced as the peak input acceleration increases. This is indicative of the increasing hysteretic damping in the foundation. The damping values plotted in Figure 10c are for steady state cycling around moment-rotation loops of fixed rotation amplitude and so are not directly relevant to the damping obtained during an earthquake record. Pender et al. (2017), reporting an investigation of the performance of multi-storey buildings on shallow foundations having a hyperbolic moment-rotation curve, calculated numerically the SDOF response to snap-back release from various initial displacements. This revealed that there was considerable damping in the first half cycle of response and then a gradual reduction in damping.

The spectra in Figure 14 are dominated by the response of the 10 storey elastic structure supported on the nonlinear foundation. One might have expected, with the larger values of the scale factor, some period lengthening of the peak response because of nonlinearity in the foundation. From Figure 12c we see that the peak foundation rotation during the motion when the scaling factor is 2 is about 1 milli-radian; if this is the peak rotation then the rotations for the remainder of the response will be smaller. Referring to Figure 10b the equivalent stiffness for a rotation amplitude of 1 milli-radian is about 90% of the elastic value. From equation 1 the period of the structure foundation system for elastic behavior 1.04 seconds, when 0.9 of the elastic foundation rotational stiff-

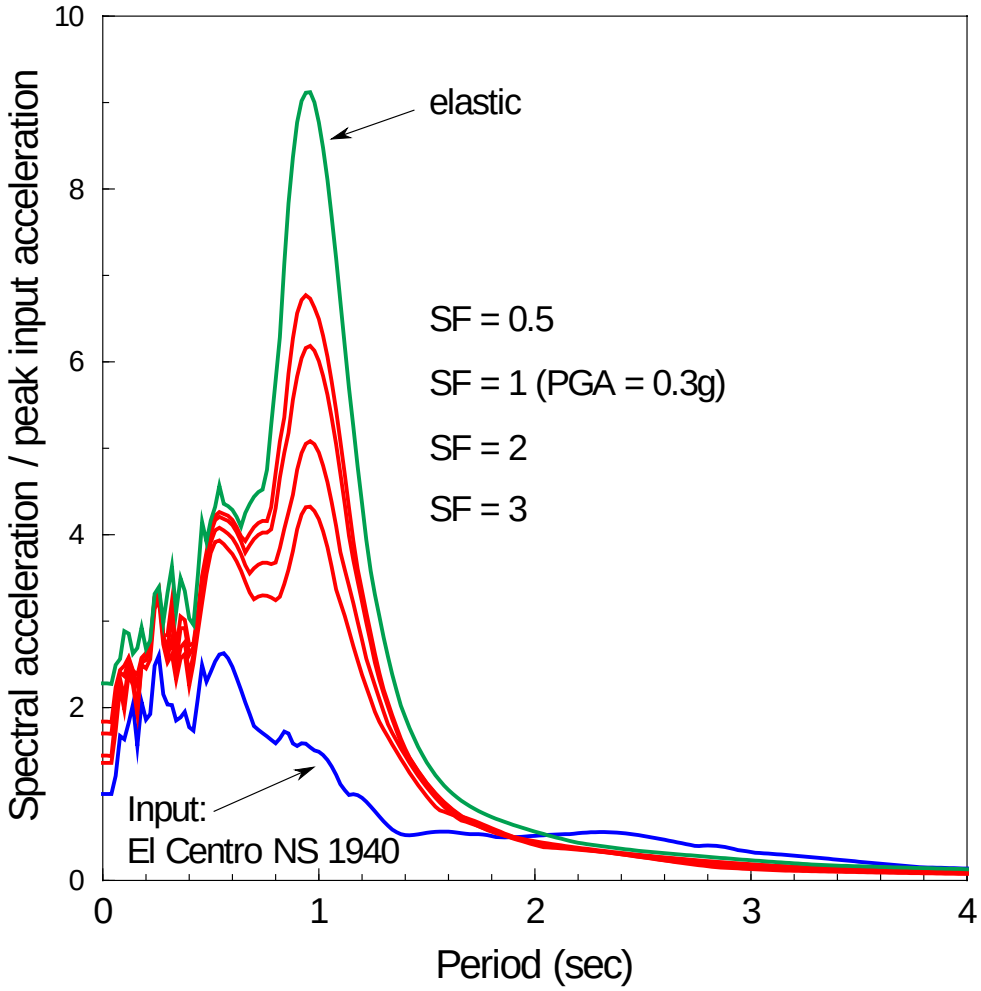

Figure 14 *Response spectra, normalised with respect to the peak input acceleration, for the calculated horizontal acceleration of the SDOF mass to the scaled 1940 N-S El Centro record. The scale factors for the input ranged from 0.5 to 3.0, with the PGA for a scale factor of 1 being 0.3 g.*

ness is used the period is lengthened by 0.05 seconds. Given this, it is not surprising that the peaks of the response spectra for the SDOF mass are close to the 1 second period of the above ground 10 storey elastic structure. Figure 12 shows that, despite the small foundation rotations, there is still hysteretic damping and it is this damping that reduces the peaks in the response spectra as the scale factor is increased. In other words the hysteretic damping absorbs some of the incoming energy and prevents it being passed upwards into the elastic structure.

7 Conclusions

The motivation for the development of a one dimensional shallow foundation macro-element in this chapter is three-fold: first, to use the structural engineering substitute structure concept but in a different context where the

nonlinearity occurs in the foundation rather than the above-ground elastic structure (Figures 2 and 3); second, to make things as simple as possible to ease sensitivity studies during the design process; third, to look specifically at situations dominated by rotational response of the foundation where settlement and sliding can be ignored. The following conclusions are reached:

- Small foundation rotations have a significant effect on the response not because of reduced stiffness but because of hysteretic damping, Figure 12.
- The foundation moment-rotation response is controlled by the vertical load which means that the section of the bearing strength surface at the vertical load carried by the foundation must be considered in estimating M_u, Figure 11 and equation (6).
- The continuous curvature of the hyperbolic curve means that plastic yielding of the foundation does not occur, rather the relationship is a type of hypoplasticity.
- Uplift is not considered specifically in the macro-element presented herein, but it is recognised that it is an important part of the explanation for the shape of the foundation moment-rotation curve.
- The rotation dependent equivalent stiffness and hysteretic damping of the model follow the expected trends, Figure 10 b and c.
- By altering the stiffness immediately after a change in direction of the rotation the amount of hysteretic damping can be controlled, Figures 8 and 9.
- The hysteretic damping in the foundation shields the supported elastic structure from some of the incoming earthquake energy, Figure 14.

8 References

Algie, T. B., Pender, M. J. and Orense, R. P. (2010). Large scale field tests of rocking foundations on an Auckland residual soil, In: *Soil Foundation Structure Interaction* (R Orense, N Chouw, and M Pender (eds.)), CRC Press / Balkema, The Netherlands, pp. 57- 65.

Algie, T. B. (2011). Nonlinear Rotational Behaviour of Shallow Foundations on Cohesive Soil, Ph D thesis, University of Auckland.

Anastasopoulos, I., Gazetas, G., Loli, M., Apostolou, M., and Gerolymos, N. (2010). Soil failure can be used for seismic protection of structures. *Bulletin of Earthquake Engineering*, 8(2): 309 – 326.

Anastasopoulos, I. & Kontoroupi, Th. (2014). Simplified approximate method for analysis of rocking systems accounting for soil inelasticity and foundation uplifting. Soil Dynamics and Earthquake Engineering, 56, pp. 28-43.

Carr, A. (2016) Ruaumoko. Carr Research Ltd., Christchurch, New Zealand.

Chatzigogos, C. T., Pecker, A. & Salençon, J. (2007). A macro-element for dynamic soil-structure interaction analyses of shallow foundations. 4th Int.

Conf. on Earthquake Geotechnical Engineering, Thessaloniki, Greece, June 25-28.

Chatzigogos, C. T., A. Pecker, and J. Salenc¸on (2009). Macroelement modeling of shallow foundations. Soil Dynamics and Earthquake Engineering 29, 765–781.

Clough, R. W. & Penzien, J. (1993). *Dynamics of Structures*, 2nd ed., McGraw-Hill, New York.

Cremer, C., A. Pecker, and L. Davenne (2001). Cyclic macro-element for soil-structure interaction: material and geometrical non-linearities. International Journal for Numerical and Analytical Methods in Geomechanics 25(13), 1257–1284.

Cremer, C., A. Pecker, and L. Davenne (2002). Modelling of nonlinear dynamic behaviour of a shallow strip foundation with macro-element. Journal of Earthquake Engineering, 175–211.

Dassault Systemes. (2010). Abaqus 6.8-EF2. Vélizy-Villacoublay, Ile-De-France, France.

Deng, L., Kutter, B., and Kunnath, S. (2014). Seismic Design of Rocking Shallow Foundations: Displacement-Based Methodology. *J. Bridge Eng.*, 19 (11) DOI: 10.1061/(ASCE)BE.1943-5592.0000616.

Duncan, J. M. and Chang, C. Y. (1970). Nonlinear analysis of stress and strain in soils. Proc. ASCE, Jnl Soil Mechanics and Foundations Division, 96 (SM5), 1629-1653.

Figini, R., R. Paolucci, and C. T. Chatzigogos (2012). A macro-element model for non-linear soil-shallow foundation-structure interaction under seismic loads: theoretical development and experimental validation on large scale tests. Earthquake Engineering & Structural Dynamics 41(3), 475–493.

Gajan, S. and Kutter, B.L. (2008). Capacity, settlement, and energy dissipation of shallow footings subjected to rocking. *Journal of Geotechnical and Geoenvironmental Engineering*, ASCE, 134(8): 1129–1141.

Gazetas, G. (2015). Avoiding Over-Conservatism and Conventional Dogmas in Seismic Geotechnical Design**.** Keynote address, 12th Australia-New Zealand conference on Geomechanics, Wellington, February.

Ishihara, K. (1996). *Soil behaviour in earthquake geotechnics*. Oxford Science

Kelly, T. E. (2009). Tentative seismic design guidelines for rocking structures, *Bulletin of the New Zealand Society for Earthquake Engineering*. 42 (4). 239-274.

Kondner, R. L. (1963). Hyperbolic stress-strain response: cohesive soils. Proc. ASCE, Jnl. Soil Mechanics and Foundations Division, 89 (SM1), 115-143.

Loli, M., Knappett, J. A., Brown, M. J., Anastasopoulos, I. & Gazetas, G. (2015) Centrifuge Testing of a Bridge Pier on a Rocking Isolated Foundation Supported On Unconnected Piles. Proc. 6th ICEGE, paper 362, Christchurch, November.

Millen, M. (2015). Integrated performance-based design of building-foundation systems. PhD thesis, University of Canterbury.

Panagiotidou, A. I., Gazetas, G. and Gerolymos, N. (2012). Pushover and Seismic Response of Foundations on Stiff Clay: Analysis with P-Delta Effects. Earthquake Spectra, 28(4), 1589-1618.

Pecker, A. and Teyssandier, J.-P. (1998). Seismic design for the foundations of the Rion Antirion bridge. Proc. Instn. Civil Engrs. Geotechnical Engineering, 131 (Jan.), 4 – 11.

Pender, M. J. (2007) Seismic design and performance of surface foundations. Chapter 10, *Earthquake Geotechnical Engineering*, K. D. Pitalakis (ed), Springer, 215-241.

Pender, M. J., Algie, T. B., Storie, L. B. and Salimath, R. (2013). Rocking controlled design of shallow foundations, *Proc. 2013 NZ Society for Earthquake Engineering Conference*, Wellington.

Pender, M. J. (2017). Bearing strength surfaces implied in conventional bearing capacity calculations. *Geotechnique*, 67(4), 313-424, DOI: 10.1680/geot./16-P-024.

Pender, M. J., Algie, T. B., Storie, L. B. and Salimath, R. (2017). One dimensional moment-rotation macro-element for performance based design of shallow foundations. Proceedings Performance Based Design III (PBDIII), Vancouver.

Plaxis. 2012. Plaxis 3D – Version 2012, Plaxis b.v. The Netherlands.

Priestley, M. J. N., Calvi, G. M. and Kowalsky, M. J. 2007. *Displacement-Based Seismic Design of Structures*, IUSS Press, Pavia, Italy.

PTC (2015). Mathcad 15 (M045). PTC Corporation, Needham, MA, USA.

Salimath, R (2017) Experimental and finite element study of moment-rotation response of shallow foundations on clay, PhD thesis, University of Auckland.

Shibata, A. and Sozen, M. (1976). Substitute structure method for the seismic design in reinforced concrete, *Journal of Structural Engineering*, Vol. 102(1), pp. 1-18.

Storie, L. B., Knappett, J. A. and Pender, M. J. (2015). Centrifuge modelling of the energy dissipation characteristics of mid-rise buildings with raft foundations on dense cohesionless soil. Proc. 6th International Conference on Earthquake Geotechnical Engineering. Christchurch, New Zealand.

Storie, L. B (2017). Soil-foundation-structure interaction in the earthquake performance of multi-storey buildings on shallow foundations. PhD thesis, University of Auckland.

Toh, J. C. W. (2008). Performance based aseismic design of shallow foundations. ME thesis, University of Auckland.

Toh, J. C. W. and Pender, M. J. (2010). Design approaches and criteria for earthquake-resistant shallow foundation systems. In: Soil-Foundation-Structure-Interaction (R. P. Orense, N. Chouw, and M. J. Pender (eds.)), CRC Press/Balkema, The Netherlands, pp. 173-180.

Wolf, J. P. (1985). *Dynamic Soil-Structure Interaction*. Prentice Hall, New Jersey, USA.

Wolf, J. P. and Deeks, A. J. (2004). *Foundation vibration analysis: a strength of materials approach.* Elsevier, Oxford, UK.